Spot events detection along a large scale sensor based on ultra weak FBGs using time-frequency analysis

Amelia Lavinia Ricchiuti* and Salvador Sales

Optical & Quantum Communications Group, iTEAM Research Institute, Universidad Politécnica de Valencia (UPV), Valencia 46022, Spain
**Corresponding author: amric1@iteam.upv.es*

Received 29 October 2015; revised XX Month, XXXX; accepted XX Month XXXX; posted XX Month XXXX (Doc. ID XXXXX); published XX Month XXXX

A simple scheme for interrogating a 5 m-long photonics device and its potential applications to quasi-distributed fiber sensing is proposed. The sensor consists of an array of 500 identical very weak fiber Bragg gratings (FBGs). The gratings are 9 mm-long and have been serially written in cascade along a single optical fiber. The measurement system is based on a combination of optical time domain reflectometry (OTDR) and frequency scanning of the interrogating pulse. The time-frequency analysis is performed by launching an optical pulse into the sensor and by retrieving and analyzing the back-reflected signal. The measurement of the temperature, length and position of spot events along the sensors is demonstrated, with good accuracy. As both spatial and temperature resolution of the method depend on the input pulse duration, the system performance can be controlled and optimized by properly choosing the temporal duration of the interrogating pulse. A spatial resolution of 9 mm (ultimately dictated by one grating length) has been obtained with an 80 ps optical pulse; while a temperature resolution of less than 0.42 K has been demonstrated using a 500 ps incident pulse. The sensor proposed proves to be simple, robust, polarization insensitive and alleviates the instrumentation complexity for distributed sensing applications.

OCIS codes: *(060.3735) Fiber Bragg gratings; (060.2370) Fiber optics sensors; (280.4788) Optical sensing and sensors; (280.6780) Temperature.*

http://dx.doi.org/10.1364/AO.99.099999

1. INTRODUCTION

Over the years, fiber optic devices have turned into one of the core technologies in a variety of sensing applications due to their advantageous characteristics such as simplicity, small size, light weight, low insertion loss, low cost, and the ability to make multiple distributed measurements along the fiber length. Furthermore, since optical fibers are made of dielectric material, they are non conducting, immune to electromagnetic interference (EMI), chemically inert, spark free and extraordinarily resistant to corrosive environments [1]. All these attractive characteristics are highly desirable for remote interrogation from long distance and/or in harsh environments.

Recently, distributed optical fiber sensors have attracted growing interest in sensor technology as they present the key advantage that the entire optical fiber itself can be turned into a linear sensing element. Distributed fiber optic sensors are implemented by analyzing back-reflected light that occurs uniformly along the fiber. Those methods, based on elastic optical effects (Rayleigh) [2] or inelastic optical effects (Brillouin and Raman) of the back-scattered light, enable strain, temperature and vibration sensing over long range with relatively sharp spatial resolution [3], [4].

On the other hand, fiber Bragg gratings (FBGs) based devices have been playing a key role in sensing area applications owing to their fast response, high sensitivity, distributed and multiplexing capability of measuring different kinds of physical and mechanical parameters [5]. Furthermore, FBG sensors present some crucial advantages when compared to methods based on elastic/inelastic scattering. Fundamentally, a FBG does not isotropically radiate the light from the activating pulse like in a scattering process, but returns it unidirectionally back into the fiber like a partial reflector [6]. This multiplies the efficiency of the process, with the consequence that the systems employed to interrogate FBG sensors do not require very high pump power to be launched in the sensing fiber, avoiding therefore the onset of non-linear effects which may negatively affect the measurements. This also results in very simple and cost-effective interrogation systems with comfortable signal-to-noise ratios. However, FBG sensors normally only supply information at discrete points; for this reason, FBGs-based devices have been largely employed to perform highly sensitive discrete point sensing. Nevertheless, a substantial added value is offered by fully distributed sensing, in which the entire length of the fiber generates information. Preliminary proposals have been demonstrated to characterize the Bragg frequency distribution along a FBG, in order to realize distributed temperature/strain sensors. In this scenario, the optical low-coherence reflectometry (OLCR) technique [7] has demonstrated very good performance in terms of spatial resolution. However, the OLCR scheme presents a limited measurement range and a slow response time. Another approach is based on the synthesis of optical coherence function (SOCF) [8], which allows a point-by-point characterization of the grating properties by simply tuning the modulation frequency of the optical source. Anyway, this technique requires a very complicated setup and expensive devices. A third alternative for distributed measurements along optical fibers has been proposed based on optical frequency domain reflectometry (OFDR) [2]. This approach enables temperature and strain measurements over long ranges with very good performance in terms of spatial resolution and precision. This performance has been obtained by combining OFDR with an advance cross-correlation based method, which comprises a sophisticated post processing scheme and an auxiliary interferometer used to avoid any non-linearity. Moreover, the systems results polarization-dependent and thus requires the presence of a polarization beam splitter and two separate photo-detectors to mitigate signal fading.

Subsequently, fiber distributed sensing based on very-weak reflectivity FBG was also demonstrated using optical time-domain reflectometry (OTDR) [9]. By scanning the laser frequency a distribution map of the reflectivity along the fiber has been obtained, demonstrating very good performance in terms of accuracy and signal response.

Starting from the idea presented in [9], we decided to move toward the possibility to apply a very long FBG as a large-scale distributed sensing device. For a long range sensor, ultra weak gratings are required, which ensures low crosstalk level among units in the array and allows the propagation of the optical incident signal over the entire length of the sensor. Since fabricating a long, continuous and homogenous FBG with no phase hopping and with very low reflectivity is an expensive and complicated issue, with a maximum reported length of 1 m [10], we propose a sensor made of an array of 500 identical very-weak FBGs written in cascade and covering 5 m of optical fiber. The measurement system is essentially based on a combination of frequency scanning of the interrogating pulse and OTDR technique [11].

The possibility of using weak reflectors written in cascade along a single optical fiber for sensing applications has attracted the interest of some research groups. For instance, in [12] a quasi-distributed fiber optic sensor based on multiple interferometers built from pairs of arbitrary weak reflectors was investigated. Inspired by the operation principle of microwave photonics (MWP) filters, Huang et al. proposed an optical carrier based microwave interferometry scheme for sensing application, demonstrating high signal quality and polarization-insensitive measurements. However, the method requires a weighty post-processing analysis including a complex and inverse Fourier transform of the microwave spectrum, a time-gating to the time-domain signal and hence a Fourier transform of the gated signal to obtain the final microwave interferogram. Besides, an interrogation scheme based on a combination of time-division multiplexing (TDM) and wavelength-division multiplexing (WDM) technique for large range sensing based on an array of identical ultra-weak FBGs was demonstrated [13, 14]. Large-scale networks composed of several hundreds of serial FBGs with a couple of meters equidistance between two adjacent gratings were interrogated by using a 20 ns pulse, demonstrating the feasibility to integrate several hundreds of FBG in a single optical fiber for sensing application. Anyway, these configurations present a huge dark zone between consecutive sensing elements (couple of meters), hence, as a non-distributed sensing scheme, the system can only monitor and detect events at the positions where the FBGs are located while whatever happens in the dark zone between gratings remains unavoidably undetected.

In this contribution, a quasi-distributed sensor based on an array of 500 equal low reflectivity FBGs spaced by ∼ 1 mm is employed and a time-frequency domain analysis is performed, enabling the detection of spot events along the cascade sensing device. The most common approach to interrogate a FBG cascade sensor is to use optical pulses much shorter than the transit time of the light through two consecutive sensing elements [13, 14]. In this way, it is ensured that the optical pulse travelling along the FBGs chain one grating at the time, leads to no overlapping between back-scattered signals coming from adjacent FBGs. This allows stable and fluctuation-free time waveforms to be detected at the oscilloscope and eventually post-processed. In the case of physical separation of few mm between sensing units along a large-scale network, ultra-short optical pulses are necessary to avoid any overlapping between back-scattered signals coming from different gratings. Anyway, the ultra-short pulse requirement unavoidably enhances the setup layout and system cost and complexity. In practical terms, to obtain an optical pulse width of few tens of ps by modulating a continuous wave laser source, a signal generator of some tens of GHz is necessary. On the other hand, complex and bulky configurations, like a nonlinear optical loop mirror [11], were employed to temporally compress the input optical pulse. This demonstrates the existence of a clear trade-off between the minimum value of physical separation between gratings and the interrogating pulse width. In contrast, this work shows the possibility to interrogate a weak FBG cascade sensor using optical pulses having duration longer than the transit time through consecutive FBGs. Under these conditions, the input pulse will cover several gratings at one time; hence giving rise to coherent effects during the measurement process. Despite the presence of these coherent interferences, the detection of the position and length of spot events along the sensor is demonstrated with good performance in terms of measurand resolution. Both the spatial and temperature resolution of the system can be controlled by opportunely choosing the temporal duration of the interrogating pulse. The proposed quasi-distributed sensor proves to be robust and polarization insensitive, releasing the instrumentation complexity and drastically simplifying the setup layout as the requirement for ultra-short optical pulses is alleviated.

2. MEASUREMENT SETUP

The photonic sensor is composed of an array of 500 identical ultra-weak (reflectivity ≈ 0.001) FBGs. These gratings are 9 mm-long and are spaced by ∼ 1 mm, so that the total sensor length is 5 m. This is the same previously used device interrogated by a MWP filtering technique [15]. The setup used here to interrogate the weak FBG cascade sensor is illustrated in Fig. 1. The output of a tunable laser source is shaped as a pulse train with a repetition rate t_p chosen to be longer than the transit time of the light through the sensing device. This way, it is secured that a single pulse is present along the entire length of the 5 m-long sensor, preventing crosstalk between adjacent incident pulses. As a result, a Gaussian-shaped optical pulse having temporal duration τ is launched into the device under test (DUT) through an optical circulator. Finally, the back-reflected signal from the DUT is acquired by an oscilloscope and analyzed via a computer. The other end of the DUT is left open in the air to provide a reflection signal that will be used as a reference point to localize the position of the spot event along the FBG-based cascade sensor.

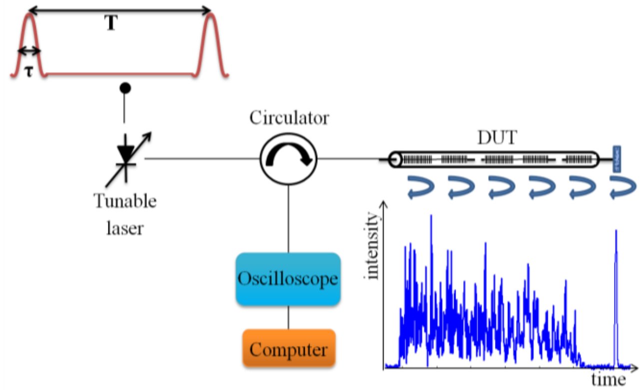

Fig. 1. Experimental layout to interrogate the weak FBG based sensor.

When the input pulse is launched into the photonics sensor composed of low reflectivity FBGs, it is continuously back-reflected while propagating through the entire DUT length. By controlling the central wavelength of the incident pulse, the detection of spot events can be achieved, with a spatial resolution dictated by half the input pulse duration, like any OTDR technique [9]. The here reported measurements show that such a system can offer an attractive, robust and cost-effective approach for quasi-distributed fiber sensing.

3. EXPERIMENTAL MEASUREMENTS AND RESULTS

The signal used to characterize the Bragg frequency distribution of the FBG cascade sensor is a train of 500 ps-long optical pulses with a repetition rate of 64 ns. As the DUT is 5 m-long, the round-trip time of the light over its length is around 50 ns. The pulse rate repetition t_p = 64 ns ensures the absence of overlapping between back-reflected signals from successive incident pulses. It is worth mentioning that the pulse temporal duration τ = 500 ps is almost equivalent to the transit time through 10 weak FBGs of the array, since the separation between two consecutive 9 mm-long gratings is ~ 1 mm. The back-reflected signals coming from adjacent FBGs are mixed together at the detection stage. These contributions from different gratings will randomly sum up or subtract one another (i.e. with random phase hops). Hence, this produces, in turn, two undesirable side effects: waveform instability and intensity fluctuations. However, as far as the first issue is concerned, initial measurements have revealed a slight instability of the traces recovered by the oscilloscope; this problem is easily overcome by averaging 20 repeated traces, allowing clear and stable measurement waveforms. On the other hand, intensity fluctuations of the time waveform due to random phase hops between adjacent gratings have been observed, causing the rising of dead-zones in the reflected signal. Nevertheless, in our experiments, the length and position of the spot event can be measured starting by its time waveform duration, which is the difference between the final instant and the initial one, as it will be described in the next section. The intensity fluctuations of the time waveform, however, only affects the inner zone between the rise and fall slopes, while the two transition sides of the time-waveform (i.e. rise and fall slopes) remain unchanged. This infers that, despite the presence of these dead-zones in the time-domain traces, it does not impede the measurements of the position and length of the spot events.

Figure 2(a) shows the time response of the sensor when the central frequency of the tunable laser matches the Bragg frequency and the aforementioned train of pulses is launched into the sensing device. Due to the weak reflectivity of the 500 FBGs contained in the DUT, a small fraction of the signal pulse experiences a back-reflection along the entire length of the sensor during the propagation. Hence, the length L_{DUT} of the DUT is encoded in the reflected waveform duration t_{DUT}, according to the equation:

$$L_{DUT} = \frac{c \cdot t_{DUT}}{2n_g}. \quad \textbf{(1)}$$

being n_g is the group refractive index of the fiber and c is the speed of light in vacuum.

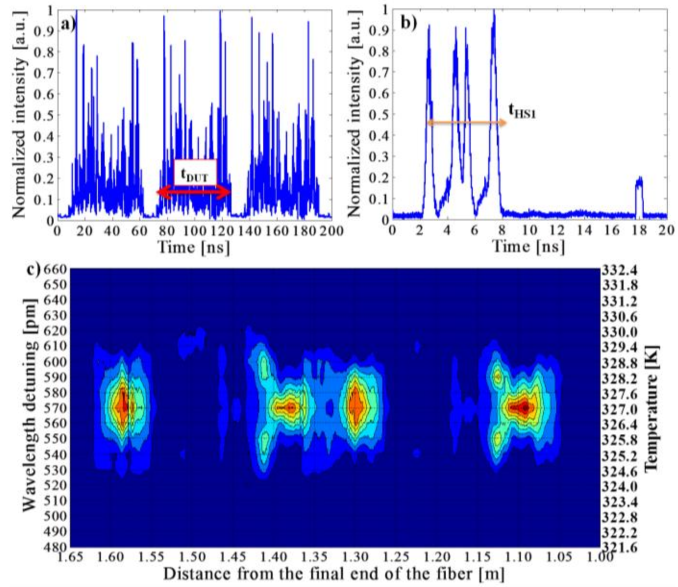

Fig. 2. Measurement set for an input pulse width of 500 ps. (a) Measured time response of the DUT. Each waveform has duration of 50 ns corresponding to the round-trip time through the 5 m-long fiber sensor. (b) Measured time response of the hot spot. (c) 3D distribution map of the back-reflected signal obtained by progressively scanning the central wavelength of the input pulse.

Then a hot zone is created by dipping a section of the DUT in a hot bath whose temperature is measured with a reference thermometer and is kept constant using a hot plate. This local change of temperature produces a local Bragg frequency shift. Now, the tunable laser is step-wise scanned and for each wavelength the time waveform is acquired by the oscilloscope and stored by the computer. At this point, the integrated intensity is calculated for each time-waveform, by simply summing up all the reflective intensity contributions. This is a very easy and cost-effective procedure as it only requires the sum of all the intensity samples avoiding sophisticated and time consuming post-processing techniques such as cross-correlation based methods. Clearly, the higher value of the integrated intensity corresponds to the waveform relevant to the laser wavelength which matches the original Bragg wavelength of the 5 m-long sensing device. Starting from this wavelength and gradually incrementing this value, a progressive reduction of the integrated intensity is observed. But, when the wavelength of the interrogating pulse is moved closer to that of the hot zone, the integrated intensity starts to rise as long as it reaches a maximum value, before decreasing again. When the maximum value is reached, the input pulse wavelength is matching the Bragg wavelength of the hot spot. The corresponding time-waveform is illustrated in Fig. 2(b): here it can be seen as, employing an interrogating pulse covering several sensing units at one time, back-reflected signals coming from adjacent FBGs will overlap at the detection stage. These contributions from different gratings will randomly sum up or subtract together, causing, in turn, the onset of coherence effects, bringing dead-zones in the measured waveforms. This is the reason why the reflected waveform from the entire DUT illustrated in Fig. 2(a) is neither repetitive not regular. Nevertheless, as previously mentioned, the presence of these dead-zones does not impede the measurements of both position and length of the hot spot, as following. The reflection at time t = 18 ns is the one delivered by the end facet of the DUT, used as a reference point. By evaluating the time duration of the hot spot waveform t_{HS1}, and by using Eq. (1), the length of the spot event is measured to be L_{HS1} = 55 cm. Similarly, the position of the heated zone along the sensor is calculated by evaluating the time separation between the reference pulse and the time-waveform relative to the hot spot, according to Eq. (1). So, the middle point of the hot spot is calculated to be 132 cm from the end facet of the fiber. At a given wavelength of the interrogating pulse, the back-reflected signal is collected; as this operation is repeated by step-wise scanning the central wavelength of the incident pulse, the 3D map representing the distributed reflection spectrum is obtained, as shown in Fig. 2(c). Concretely, the tunable laser has been swept with a 10 pm step. The laser source actually comprises wavelength reference, but anyway, even if the laser had not had it, the measurements would be performed by evaluating the wavelength detuning with respect to the central wavelength of the original DUT reflection.

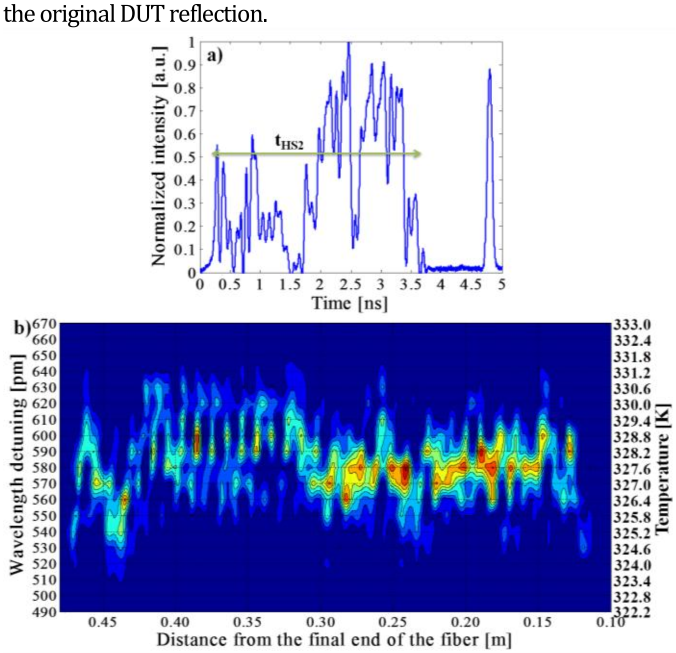

Fig. 3. Measurement set for an input pulse width of 80 ps. (a) Measured time response of the hot spot. (b) 3D distribution map of the back reflected signal obtained by progressively scanning the central wavelength of the input pulse.

Another set of measurements has been performed by using a shorter interrogating pulse, showing a temporal width of 80 ps, following the same methodology as previously described. The purpose of this second experiment is to prove that a shorter input pulse may reduce the intensity fluctuations and therefore the presence of dead-zones in the reflected signal. Once again a hot spot is applied at a certain point of the sensor and the step wise scanned procedure is repeated. Figure 3(a) shows the time-waveform corresponding to the laser wavelength which matches the Bragg wavelength of the hot zone. The reflection at time t = 4.8 ns is the one provided by the end facet of the DUT. By evaluating the time duration of the hot spot waveform t_{HS2}, the length of the spot event is measured to be L_{HS2} = 35 cm. Moreover, the middle point of the hot spot is calculated to be 29 cm from the end facet of the fiber. The distributed reflection 3D map is obtained by scanning step-by-step the central wavelength of the interrogating pulse and is illustrated in Fig. 3(b). Here it can be seen that using a shorter incident pulse dramatically reduces the number of back-reflected signals coming from adjacent FBGs which interfere together, and then the presence of dead-zones in the intensity waveforms. This means that by interrogating the sensor with an appropriately short pulse the intensity fluctuation effects can be suppressed, leading to no dead-zones in the measurement of back-reflected signals. In a similar way, the intensity ripples (and hence the dead-zones) can be suppressed by using a FBGs cascade device having enough separation between each neighboring sensing element, though presenting insensitive sections.

4. SENSOR PERFORMANCES

This section is focused on the performance that the proposed sensor presents in the measurement of the hot spot length, position and temperature.

A. Temperature Analysis

The Bragg wavelength of the proposed sensor has been precisely measured at 293.2 K room temperature when neither strain nor temperature changes have been applied on the device. In this condition, the Bragg wavelength of the DUT has been calculated to be 1549.857 nm. Also temperature measurements have been performed several times in order to narrowly define the thermal coefficient of the fiber. The measurements performed have been achieved by scanning the central wavelength of the interrogating pulse by 10 pm increments. Based on the fiber temperature coefficient, which is 16.855 pm/K, the temperature accuracy of the method is estimated to be better than 0.6 K. This is just a rough and safe approximation of the precision of the proposed method which can actually be improved by implementing standard fitting of the acquired data [16]. Also, the temperature range of the system is basically dictated by the temperature coefficient of the FBG-based sensing network and by the laser wavelength scanning range. The temperature of the hot spot can be calculated by the wavelength shift between the laser wavelength which matches the Bragg wavelength of the hot zone and the original Bragg wavelength of the DUT. In the case of the 55 cm-long hot spot of Fig. 2(b) and (c) the wavelength shift has been measured to be 570 pm. By using the temperature coefficient, the measured temperature shift results to be 33.8 K. By adding this value to the room temperature, the temperature of the hot spot is calculated to be 327.0 K. The temperature of the hot bath is measured with a reference instrument to be 326.7 K, giving a temperature error of 0.3 K, which results to be below the value of the estimated accuracy.

Temperature measurements have also been performed for the 35 cm-long hot spot of Fig 3(a) and (b). In this case, the measured wavelength shift is 580 pm, leading to a temperature shift of 34.4 K, which in turn gives a calculated hot spot temperature of 327.6 K. The temperature of the hot bath measured by the reference thermometer is 327.4 K, demonstrating a temperature error of 0.2 K, in agreement with the predicted accuracy of 0.6 K.

Besides, the temperature resolution of the configuration essentially derives from the width of the input pulse spectrum, which in turn depends on the pulse temporal duration τ. In case of Gaussian-shaped pulse, the pulse spectral width Δf is given as $\Delta f = (2ln2/\pi)/\tau \approx 0.441/\tau$ [9]. For a 500 ps-long pulse, this leads to a pulse spectral width of 7.056 pm which corresponds to a temperature resolution of less than 0.42 K. Whereas, for τ = 80 ps, the pulse spectral width is 44.1 pm, corresponding to a temperature resolution of less than 2.62 K.

B. Spatial Resolution

As previously mentioned, the spatial resolution of the method is dictated by half the pulse duration, like any OTDR technique. To corroborate this fact, the time waveform reflected by the end facet of the sensor left open in the air is retrieved and analyzed for different pulse widths, as depicted in Fig. 4(a) and (b).

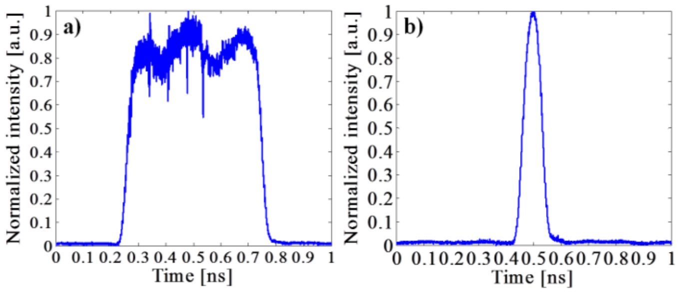

Fig. 4. Measured reflection signal provided by the end-facet of the FBG cascade fiber sensor for different widths of the interrogating pulse. (a) 500 ps. (b) 80 ps.

By using Eq. (1) the spatial resolution is calculated to be less than 5 cm in the case of a pulse width of 500 ps and less than 8 mm for a pulse width of 80 ps. The latter is just a theoretical estimation, as the ultimate limit for the spatial resolution is basically dictated by the length of the single sensing element, which actually is 9 mm.

These results provided in these 2 latter sub-sections confirm the clear expected trade-off between spatial resolution and temperature resolution of the proposed method.

C. Length and Position Calculation

As previously described, the length of the spot can be measured by estimating its time waveform duration, which is the difference between the final instant and the initial one. In case of "ideal" time waveform the rise (fall) slope of the trace would be perfectly vertical and it would take only one value for the starting (ending) instant. It is not the case for the measurements reported here. This is mainly because of the fact that the interrogating signal is a Gaussian-shaped pulse not a rectangular pulse. Figure 5 shows a measured time response for a 2 cm-long hot spot, obtained with a pulse width of 80 ps. The length and the position of the hot spot have been calculated utilizing as initial and ending points those marked with orange stars. These symbols represent the middle points of the rise and the fall edges of the trace. Also, the time values corresponding to the two extremities of both edges have been retrieved: t_a and t_b for the rising edge, t_c and t_d for the falling edge.

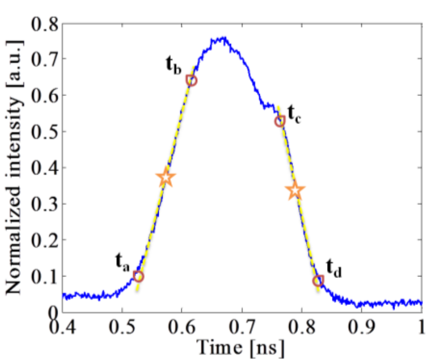

Fig. 5. Measured time response for a 2 cm-long hot spot, obtained by using an 80 ps incident pulse.

The error on the evaluations of length and position of the hot spot can be estimated, according to:

$$Err = \frac{\max[L(t_b - t_a), L(t_d - t_c)]}{2}. \quad \textbf{(2)}$$

where $L(t_b\text{-}t_a) = [(t_b\text{-}t_a)c]/(2n_g)$, $L(t_d\text{-}t_c) = [(t_d\text{-}t_c)c]/(2n_g)$ and the factor 2 is associated to the fact that the middle points of the slopes have been used to determine both the length and the position. In this way, the error has been estimated to be less than 5 mm. Similarly, these calculations have been repeated for the measurement set obtained with an input pulse width of 500 ps. In this configuration, the error has been evaluated to be less than 1 cm. This means that a broader interrogating pulse not only increases the spatial resolution but also the error made in measuring the length and the position. Anyway, it is worth pointing out that the error committed in the spatial measurements presents a value closer to that of the spatial resolution reported in the previous section, and hence it does not negatively affect the estimation of the system spatial resolution.

D. Two Spot Events Sensing

The proposed method also shows its capability for detecting two spot events even when they have the same temperature. For a large-scale sensor network, very low reflectivity of the sensing units results absolutely necessary, ensuring a low cross-talk level among identical sensors in the array and hence allowing the detection of several spot events even if they are at the same magnitude [15].

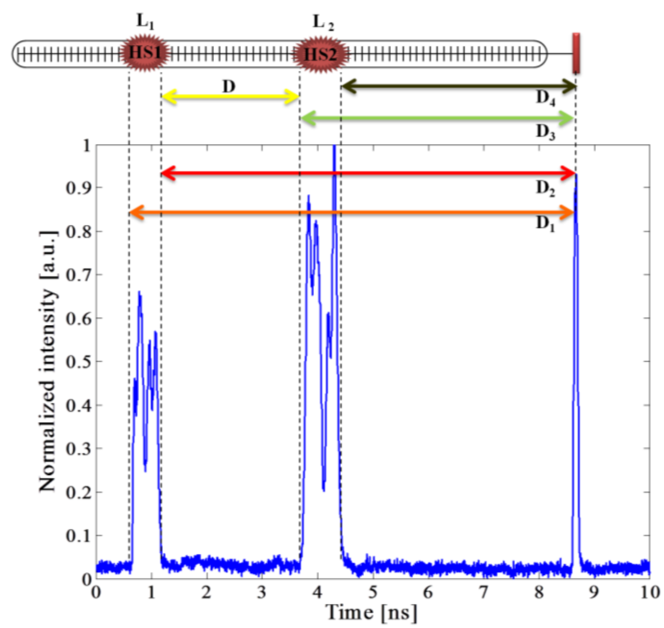

Fig. 6. Measured time response when two hot spots are provoked along the sensor. The hot spots present different length but same temperature.

In the case of the sensor presented in this contribution, to demonstrate this, two different sections of the DUT have been dipped in the hot bath. Figure 6 shows the time-waveform corresponding to the laser wavelength which matches the Bragg wavelength of the hot zones. The reflection at time $t = 8.7$ ns is the one provided by the end facet of the DUT left open in the air. By using Eq. (1), the lengths of the spot events are measured to be L_1 = 5 cm and L_2 = 6 cm, respectively. Moreover, the positions of the heated zones are calculated by evaluating the time separations between the reference pulse and the time-waveforms relating to the hot spots, according to Eq. (1). The initial and the final position of the first hot spot referred to the end-facet of the sensor (see Fig.

5) has been evaluated to be D_1 = 83 cm, and D_2 = 78 cm, respectively. Likewise, the initial and the final positions of the second hot spot referred to the end facet of the sensor have been calculated to be D_3 = 51 cm and D_4 = 45 cm, respectively. The measured separation between the two hot spots is D = 27 cm.

5. CONCLUSION

In this work the possibility to measure the local spectral characteristics along a very weak FBG-based cascade sensor has been presented and experimentally validated. The measurements have been performed by implementing a time-frequency domain analysis as demonstrated before in [9, 11], combining the OTDR technique with the frequency scanning of the interrogating pulse. However, since the fabrication of a long continuous, ultra weak and homogenous FBG is an expensive and complicated issue, here we have proposed a sensor made of an array of 500 identical ultra weak FBGs written in cascade and covering 5 m of optical fiber, with the purpose of enhancing the measurement range. An optical pulse has been sent into the sensor and the back-reflected signal has been retrieved and analyzed. This way, the time waveforms obtained by progressively incrementing the input pulse wavelength and the reflection provided by the end facet of the sensor left open in the air have been used to detect the length and the position of the hot spots located at a certain point of the sensing element. It is worth to noting that he most common approach to interrogate an ultra weak FBGs sensing network is to use optical pulses much shorter than the transit time of the light through two adjacent sensing units [13, 14], so avoiding overlapping between back-scattered signals coming from neighboring FBGs. Nevertheless, in this paper, we have demonstrated the possibility of interrogating a large-scale FBG-based sensor using pulses greater than the transit time of the light through consecutive gratings. This alleviates the requirement for ultra-short optical pulses and hence reducing the cost and complexity of the interrogation system. Firstly, a 500 ps optical pulse has been employed, giving rise to substantial random coherent effects during the measurement process. Despite the presence of these interferences, which in turn causes dead-zones over the acquired traces, the detection of the position and the length of spot events along the sensor has been demonstrated, as a proof-of-concept. In a second set of measurements, an 80 ps optical pulse has been used, in order to demonstrate that a shorter input pulse may reduce the intensity fluctuations and therefore the presence of dead-zones in the reflected signal, without negatively affecting the performance of the method in terms of stability, temperature/spatial accuracy and resolution. In particular, the resolution of the system is only dictated by the interrogating pulse duration. It turns out anyway that the dead-zones limitation can be only totally overcome by interrogating the sensor with an appropriately short pulse or by using a FBG cascade device having enough separation between neighboring sensing elements. These are complementary researches requiring further studies going beyond the scope of this paper. Furthermore, the temperature of the spot event has been calculated with an estimated accuracy of less than 0.6 K. This rough approximation can certainly be improved by implementing standard fitting techniques.

The spatial resolution of the proposed method comes from the interrogating pulse duration which is also responsible for the temperature resolution. In particular, the spatial resolution can be improved by compressing the interrogating pulse at the expense of the temperature resolution. Hence, there is a clear trade-off between these parameters resulting from the time-frequency fundamental duality; this means that the system performance can be controlled and suitably optimized by conveniently choosing the temporal duration of the interrogating pulse. A spatial resolution of 9 mm (ultimately dictated by one FBG length) and a temperature resolution of less than 2.62 K have been obtained with a 80 ps optical pulse; while a 5 cm spatial resolution and a temperature resolution of less than 0.42 K have been demonstrated by using a 500 ps incident pulse. Furthermore, as the measurement range is essentially dictated by the length of the sensor itself, large scale sensing network only requires a longer FBGs array (i.e. by further cascading sensing units) with no need to enhance the bandwidth in the acquisition electronics. The measurement speed of the method is principally dictated by time scanning range of the laser, by the acquisition time of the oscilloscope and by the number of sampling points acquired by the instrument in such a range.

Finally, it is worth noticing that the method can also be used to implement a crack/strain sensor. Moreover, due to the high sensitivity of the FBG spectrum to temperature and/or strain changes, the system presents great potential for the development of a simple solution for distributed fiber sensing with no need of optical pumping and/or sophisticated controlling systems. The proposed configuration proves to be cost effective, polarization insensitive, robust against environmental changes and easy to reconfigure. Furthermore, as no ultra-short optical pulses have been employed, the quasi-distributed sensors alleviates the instrumentation complexity and drastically simplifies the measurement scheme as the strength requires for obtaining ultra-short optical pulses is reduced.

Acknowledgment. The authors would like to thank Prof. Luc Thévenaz from the Institute of Electrical Engineering, École Polytechnique Fédérale de Lausanne (Switzerland) for its valuable help and discussions and FBGS International for kindly providing the FBG cascade fiber used during the experiment. This work was support by the Acción Financiada por el Ministerio de Educación, Cultura y Deporte in the framework of Programa de Campus de Excelencia Internacional VLC/Campus, by the Spanish MINECO through projects TEC2014-60378-C2-1-R, by the grant of the program SANTIAGO GRISOLÍA, and by the Research Excellency Award Program GVA PROMETEO 2013/012.

References

1. B. Culshaw, “Optical fiber sensor technologies: opportunities and perhaps pitfalls,” J. Lightwave Technol. **22**, 39-50 (2004).
2. M. Froggatt and J. Moore, “High-spatial-resolution distributed strain measurement in optical fiber with Rayleigh scatter,” Appl. Opt. **37**, 1735-1740 (1998).
3. A. Rogers, “Distributed optical-fibre sensing,” Meas. Sci. Technol. **10**, R75-R99 (1999).
4. X. Bao and L. Chen , "Recent progress in distributed fiber optic sensors", Sensors **12**, 8601-8639 (2012).
5. A. D. Kersey, M. A. Davis, H. J. Patrick, M. LeBlanc, K. P. Koo, C. G. Askins, M. A. Putnam, and E. J. Friebele, “Fiber grating sensors,” J. Lightwave Technol. **15**, 1442-1463 (1997).
6. L. Thévenaz, "Next generation of optical fibre sensors: new concepts and perspectives," Proc. SPIE **9157**, 9157AN (2014).
7. M. Volanthen, H. Geiger, and J. P. Dakin., “Distributed grating sensors using low-coherence reflectometry,” J. Lightwave Technol. **15**, 2076-2082 (1997).
8. K. Hotate and K. Kajiwara, “Proposal and experimental verification of Bragg wavelength distribution measurement within a long-length FBG by synthesis of optical coherence function,” Opt. Express **16**, 7881-7887 (2008).
9. L. Thévenaz, S. Chin, J. Sancho, and S. Sales, “Novel technique for distributed fibre sensing based on faint long gratings (FLOGs),” Proc. SPIE **9157**, 91576W (2014).

10. M. Gagné, S. Loranger, J. Lapointe, and R. Kashyap, "Fabrication of high quality, ultra-long fiber Bragg gratings: up to 2 million periods in phase," Opt. Express **22**, 387-398 (2014).
11. J. Sancho, S. Chin, D. Barrera, S. Sales, and L. Thévenaz, "Time-frequency analysis of long fiber Bragg gratings with low reflectivity," Opt. Express **21**, 7171-7179 (2013).
12. J. Huang, X. Lan, M. Luo, and H. Xiao, "Spatially continuous distributed fiber optic sensing using optical carrier based microwave interferometry," Opt. Express **22**, 18757-18769 (2014).
13. C. Hu, H. Wen, and W. Bai, "A novel interrogation system for large scale sensing network with identical ultra-weak fiber Bragg gratings," J. Lightwave Technol. **32**, 1406–1411 (2014).
14. W. Bai, H. Yu, D. Jiang, M. Yang, "All Fiber Grating (AFG): a new platform for fiber optic sensing technologies," Proc. SPIE **9634**, 6342A (2015).
15. A. L. Ricchiuti, J. Hervás, D. Barrera, S. Sales, and J. Capmany, "Microwave photonics filtering technique for interrogating a very-weak fiber Bragg grating cascade sensor," IEEE Photon. J. **6**, 5501410 (2014).
16. M. Soto and L. Thévenaz, "Modeling and evaluating the performance of Brillouin distributed optical fiber sensors", Opt. Express **21**, 31347-31366, (2013).